Wang *et al. J Mater Inf* 2024;4:24
DOI: 10.20517/jmi.2024.33

Journal of materials Informatics

Research Article

Open Access

Simple formula learned via machine learning for creep rupture life prediction of high-temperature titanium alloys

Ping Wang, Shang Zhao, Changlu Zhou, Jiangkun Fan, Bin Tang, Jinshan Li, Ruihao Yuan*

State Key Laboratory of Solidification Processing, Northwestern Polytechnical University, Xi'an 710072, Shaanxi, China.

***Correspondence to:** Prof. Ruihao Yuan, State Key Laboratory of Solidification Processing, Northwestern Polytechnical University, No.127 Youyi West Road, Xi'an 710072, Shaanxi, China. E-mail: rhyuan@nwpu.edu.cn

How to cite this article: Wang P, Zhao S, Zhou C, Fan J, Tang B, Li J, Yuan R. Simple formula learned via machine learning for creep rupture life prediction of high-temperature titanium alloys. *J Mater Inf* 2024;4:24. http://dx.doi.org/10.20517/jmi.2024.33

Received: 8 Aug 2024 **First Decision:** 21 Oct 2024 **Revised:** 29 Oct 2024 **Accepted:** 6 Nov 2024 **Published:** 20 Nov 2024

Academic Editor: Xingjun Liu **Copy Editor:** Pei-Yun Wang **Production Editor:** Pei-Yun Wang

Abstract

Creep behavior of high-temperature titanium alloys determines their service life and thereby prediction of creep rupture life is in demand due to the costly and time-consuming measurements. Machine learning (ML) has been employed to build surrogate models for creep rupture life; however, the commonly used algorithms are often black-box due to the pursuit of high accuracy. Here, we first show that multiple linear regression (MLR) can result in models or formulae with much higher accuracy than those based on typical black-box methods. Furthermore, by combining feature selection and symbolic regression, we obtain a simple and unified formula for accurately predicting the creep rupture life of high-temperature titanium alloys. The formula is learned using the short-term creep rupture life data and consists of merely three attributes, that is, the Molybdenum equivalent, the test stress and test temperature. It outperforms the MLR models and generalizes well to different testing data with varying long-term creep rupture life. The simple formula can be readily applied to new titanium alloys for predicting the creep rupture life and is easily accessible to experimentalists in the materials community.

Keywords: Machine learning, symbolic regression, creep rupture life, high-temperature titanium alloys

1. INTRODUCTION

High-temperature titanium alloys are frequently utilized in vital aerospace components because of their exceptional properties, such as high specific strength[1–4]. The durability of high-temperature structural components primarily relies on the creep behavior of alloys[5]. Plastic deformation associated with creep behavior under fixed temperature and stress can induce fracture incidents[6]. Given the costly and laborious experimental synthesis and measurement, much attention has been devoted to developing prediction methods[7,8]. Typical examples include empirical and theoretical models, as well as those based on machine learning (ML), which can expedite the assessment of creep properties[9–15].

The empirical and theoretical models can be roughly classified into two categories: time-temperature parameter (TTP) methods and creep constitutive model (CCM) methods[16,17]. These two kinds of methods have been widely employed in the estimation of creep behavior or creep rupture life[18]. For example, two TTP methods, the Larson-Miller model and Manson-Haferd model, were used to predict the creep rupture life of Inconel 740 and 740H alloys in a temperature range of 650 to 850 °C[19]. Kim *et al.* reported a modified Larson-Miller model to improve the prediction of the long-term creep rupture life of Inconel 617 above 900 °C[20]. The CCM methods, rooted in continuum mechanics and crystal plasticity theory, have also been applied in numerous scenarios. A semi-empirical model based on the damage mechanics equations, which considers the deformation mechanisms, was developed to predict the stress rupture properties of several single crystal superalloys[12]. Phenomenological models were developed to model all three stages of the anisotropic creep behavior of the nickel-base single crystal superalloy at temperatures above 1,000 °C[21]. However, both TTP and CCM methods are often limited to a small subset of materials space as the model parameters need to be fitted from experimental data.

ML techniques that are able to uncover patterns and laws underlying materials data are being increasingly applied for building prediction models of creep properties[22–28]. The commonly utilized algorithms include support vector regression (SVR), random forest (RF), and neural network, *etc.*, which are trained within dataset featured by inputs consisting of composition, processing and microstructure, and output being target property (e.g., creep rupture life)[25,29]. Venkatesh *et al.* utilized backpropagation neural networks to build an accurate surrogate model for creep rupture life prediction of Inconel 690 single-crystal superalloys at 1,000 and 1,100 °C[30]. Liu *et al.* developed a divide-and-conquer self-adaptive method that combines clustering and multiple ML algorithms such as SVR to improve the creep rupture life prediction of nickel-based single-crystal superalloys, and the R^2 reaches 0.9176[31]. We proposed a convolutional neural network-based cross-materials transfer learning strategy to optimize the creep rupture life prediction of high-temperature titanium alloys using the knowledge learned from superalloy data[32]. The ML-driven surrogate models for creep rupture life potentially outperform the empirical and theoretical methods in both accuracy and extrapolation when applied to new alloys. However, they are usually quite complex due to the "black-box" algorithms used, hindering the explanation of the prediction models and the use by experimentalists from materials community.

We achieve a simple formula for predicting the creep rupture life of high-temperature titanium alloys by combining feature engineering, multiple linear regression (MLR) and symbolic regression. Intriguingly, the formulae outperform the typically employed black-box models including RF, support vector machine, convolutional neural networks, and the automated ML method that integrates some of the above algorithms. Moreover, the formulae established using short-term creep rupture life data can generalize well to the alloys with long-term creep rupture life. The optimal formula established via symbolic regression, specifically, the sure independence screening and sparsifying operator (SISSO)[33], consists of merely three attributes, i.e., the test stress and test temperature, and the well-known Molybdenum equivalent for titanium alloys. The formula is easy to explain compared to black-box models and can be readily applied to any given new titanium alloy, making it accessible for experimentalists without requiring any ML relevant experience.

2. MATERIALS AND METHODS

2.1. Dataset and data preprocessing

The high-temperature titanium alloy dataset was manually collected from the literature[34–43]. It consists of 88 samples, each described by 25 features, including 15 chemical compositions, nine heat treatment processes, and two experimental conditions, with data distribution as shown in Supplementary Figure 1. We apply a logarithmic transformation to the target property, creep rupture life, i.e., taking log(creep rupture life) as the output of surrogate models. All the 25 features are normalized using the min-max method, as given by

$$x_{\text{norm}} = \frac{x - x_{\text{min}}}{x_{\text{max}} - x_{\text{min}}}, \tag{1}$$

where x represents a specific feature value for a given sample, and x_{max} and x_{min} are the maximum and minimum values of the same feature across all the samples, respectively.

The extrapolation ability is crucial for the surrogate models and is examined by dividing the 88 samples into training and testing sets. That is, models are trained with alloys of short-term creep rupture life and tested on those with long-term creep rupture life. To ensure the examination of extrapolation, the division includes seven categories considering the value of creep rupture life. The first division has 35 samples possessing creep rupture life (RT) > 100 h as the testing data and the left 53 as training data. Similarly, another six divisions are determined with different RT values, i.e., RT > 150 h (29 testing samples), RT > 200 h (22), RT > 300 h (14), RT > 400 h (11), RT > 700 h (8), and RT > 1,000 h (6).

2.2. ML models

The MLR and SISSO are both employed to learn formulas that relate composition, processing, and testing conditions to creep rupture life. In SISSO, arithmetic operations are first applied to the primary features to construct a feature library containing a large number of candidate features. In total, 12 operations are used: Addition (+), Subtraction (−), Multiplication (×), Division (÷), Exponentiation (e^x), Squaring (x^2), Cubing (x^3), Logarithm [log(x)], Square root ($\sqrt{x}$), Cube root ($\sqrt[3]{x}$), Inversion (x^{-1}), and Absolute value ($|x|$). Then the most important subset is selected by independently evaluating each candidate for its correlation with the target. A formula of the specified dimension can be obtained by fitting on the sparsified library. The form of the formulae learned by SISSO is given by

$$y = a_0 + a_1x_1 + a_2x_2 + a_3x_3, \tag{2}$$

where x_i is the new feature generated by combining basic features and arithmetic operations. The number of x_i determines the dimension of formulae; for example, the formula with only one new feature is termed 1D.

As a comparison, five black-box models, the RF, eXtreme Gradient Boosting (XGBoost), SVR, convolution neural networks (CNN), and automated ML (Autogluon), are used to build the surrogate models. The RF model optimizes four hyperparameters: n_estimators, max_depth, min_samples_split, and min_samples_leaf. The ranges for these parameters are 10-100 (step = 10), 10-15 (1), 2-5 (1), and 2-5 (1), respectively. For the XGBoost model, we tune eight hyperparameters, including n_estimators, max_depth, min_child_weight, gamma, subsample, colsample_bytree, reg_lambda, and reg_alpha, with ranges of [160, 170], 5-7 (1), 2-4 (1), 0.001-0.1 (0.01), 0.7-0.9 (0.1), 0.7-0.9 (0.1), [2, 3, 5, 8], and [0, 0.1]. For the SVR model, we optimize two hyperparameters, C and epsilon, with ranges of 2-8 (1) and 0.01-1 (0.01), respectively. All models above utilize grid search. The CNN comprises two convolutional layers with eight and 16 kernels of the same size 2 × 2, followed by a flattening layer and a fully connected layer with 128 dimensions. The input data is standardized to a uniform shape of 6 × 6, and the final output is directed to a single neuron for regression tasks. Autogluon is a toolkit based on existing ML algorithms, leveraging Bayesian optimization to achieve automated basic model selection and hyperparameter tuning. It utilizes a stacking strategy to train an ensemble model on the predictions of these basic models for final prediction[24,44]. We employ least absolute shrinkage and selection pperator (Lasso) regression, a linear model regularized with a penalty term, to select key features.

The performance of the surrogate models is evaluated using the mean absolute error (MAE) and the mean squared error (MSE) metrics, as given by

$$MAE = \frac{1}{n}\sum_{i=1}^{n}|\hat{y}_i - y_i|, \tag{3}$$

$$MSE = \frac{1}{n}\sum_{i=1}^{n}(y_i - \hat{y}_i)^2, \tag{4}$$

where y_i and $\hat{y}_i$ are the ground truth and predicted value of the ith sample, respectively, and n is the number of samples.

3. RESULTS AND DISCUSSION

3.1. Surrogate models for creep rupture life prediction

The surrogate models based on RF, XGBoost, SVR, CNN, Autogluon and MLR are trained with the training data and tested with the testing data. Figure 1 shows the extrapolation performance of the six models; the division with creep rupture life (RT) > 100 h as testing data is used as an example. Interestingly, the MLR model in Figure 1F performs the best compared to other black-box models, as indicated by the consistent distribution of both training and testing data points and the lowest MAE and MSE for testing data. By contrast, the models in Figure 1A-D suggest severe over-fitting. While the CNN model in Figure 1E seems moderate, it is too complex due to the use of multilayer networks and convolution kernels. Figure 2 shows the extrapolation capability of the MLR model in the seven divisions with different training and testing data. For both MAE and MSE, it is evident that the MLR model and the CNN model outperform the others in almost all the seven divisions. The low errors on testing data indicate that our surrogate models trained on alloys with short-term creep rupture life can predict those with long-term creep rupture life. This is important in practice as merely measuring the creep rupture life of low values is much time- and cost-effective. Considering that the MLP model can provide formulae for predicting creep rupture life and has performance comparable to the CNN model, we will focus on the MLP model in the following sections. It should be noted that the MLP model utilizes all the 25 features as inputs; this will inevitably lead to a quite complex formula, which still shows a black-box-like character. This then motivates us to reduce the features and obtain a more simple MLP model.

3.2. Reducing features for multiple-linear model

The Lasso regression is used to determine the key features. Lasso is an integration of a linear model with a regularized term. A key parameter is the coefficient (λ) of the regularized term and its increase will decrease the coefficient of each independent variable. All the coefficients are limited to zero once λ exceeds a critical value. The more rapid the coefficient becomes to zero, the less important the variable is. Taking the testing set with RT > 100 h as an example, the Lasso model is trained using the training data of 53 samples. Figure 3A shows the change of each feature coefficient with λ. The coefficient of the feature, 2nd_aging_temperature, is reduced to zero very quickly while those for V and Fe become zero the most slowly.

Figure 3B depicts the relationship between λ and binomial deviance, which is interpreted as the deviation between predictions and actual values under a specific λ. The left dashed vertical line around 0.001 corresponds to the Lasso model with the lowest error for the training data of 53 samples. The right dashed line means that at the corresponding λ, all the coefficients are zero. Based on the results from Lasso, in total, 11 features give rise to the optimal prediction model. Figure 3C shows the performance of the Lasso model on the training and testing data, both closely aligned along the diagonal line. The errors slightly increase compared to Figure 1F, indicating that the removal of 14 features by Lasso has little effect on the performance of the linear model. The formula resulting from Lasso is as follows:

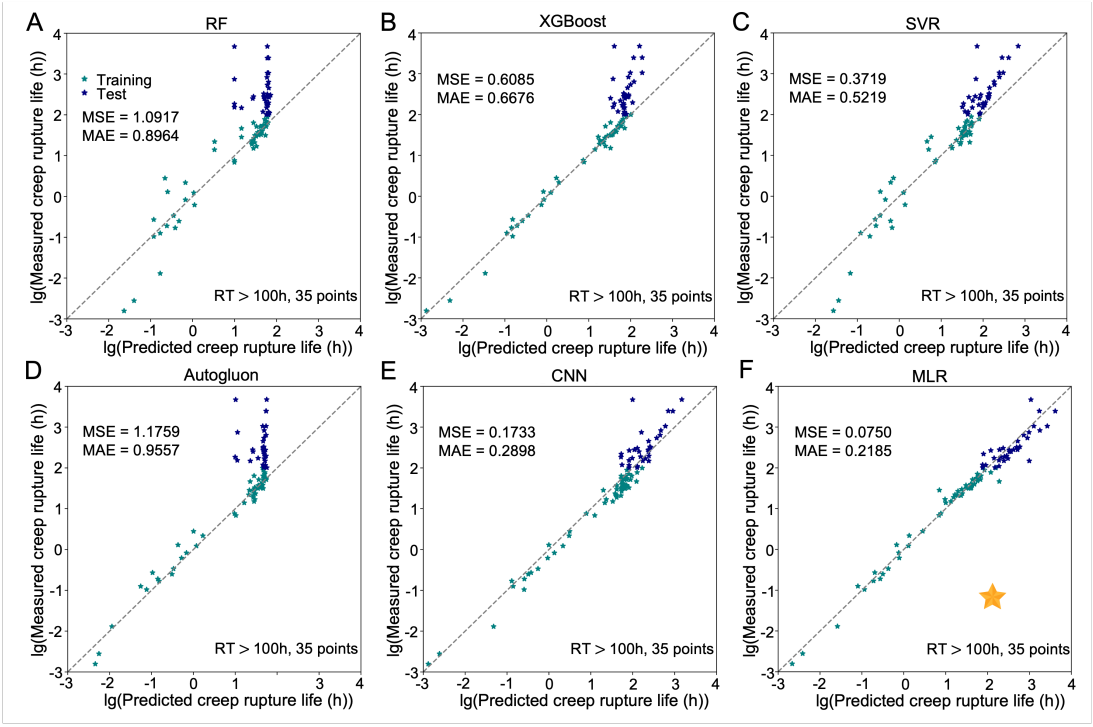

Figure 1. Extrapolation performance of the six surrogate models on both training and testing data, the data division with RT > 100 h (35 testing points and 53 training points) is used as an example. (A) RF; (B) XGBoost; (C) SVR; (D) Autogluon; (E) CNN; and (F) MLR. RT: Creep rupture life; RF: random forest; XGBoost: eXtreme Gradient Boosting; SVR: support vector regression; CNN: convolution neural networks; MLR: multiple linear regression.

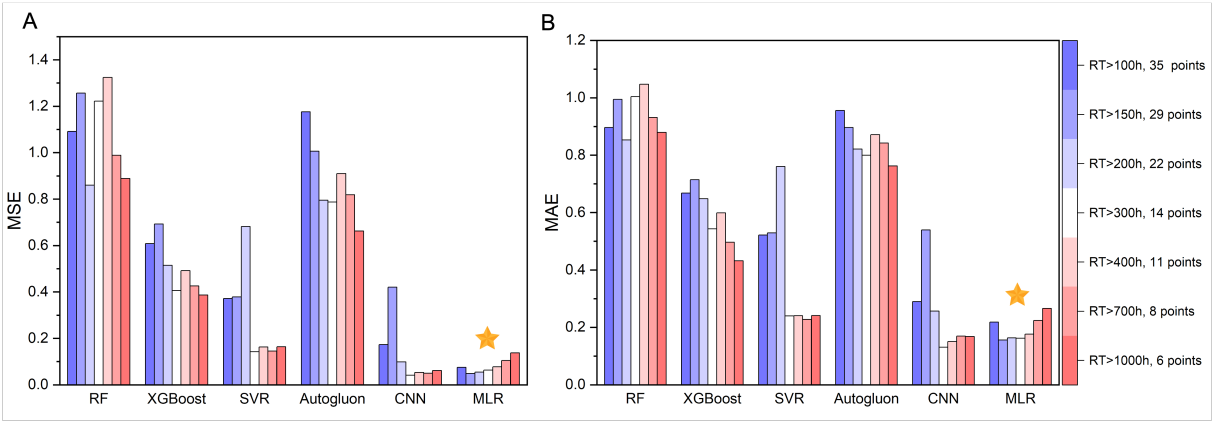

Figure 2. Comparison of model (based on 25 features) performances on different testing datasets. (A) MSE and (B) MAE. MSE: Mean squared error; MAE: mean absolute error.

$$y = 0.599solution\_time + 0.649solution\_temperature + 0.008aging\_time + 0.131C + 0.233Ni + 0.589(Nb + Ta) - 2.087V - 2.115Fe + 0.006Sn - 5.131test\_temperature - 3.751test\_stress. \quad (5)$$

A similar Lasso-based feature selection procedure is applied to the other six datasets with different divisions. For each dataset, we determine about ten features for an optimal linear model with the lowest error. To ensure the surrogate models and formulae can be generalized to different data division scenarios, we use the

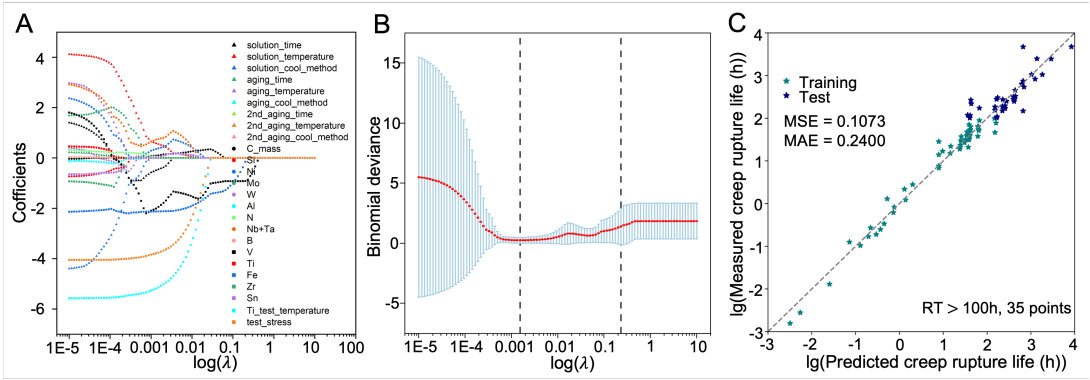

Figure 3. Feature selection via Lasso and model performance with reduced features, the data division with RT > 100 h is presented as an example. (A) Coefficient change of each of the 25 features with λ; (B) Model bias (binomial deviance) as a function of λ, the red points represent the mean value and the associated error bars are the standard deviation from multiple cross-validations; (C) The performance of the Lasso model with reduced features (11). Lasso: Least absolute shrinkage and selection pperator; RT: creep rupture life.

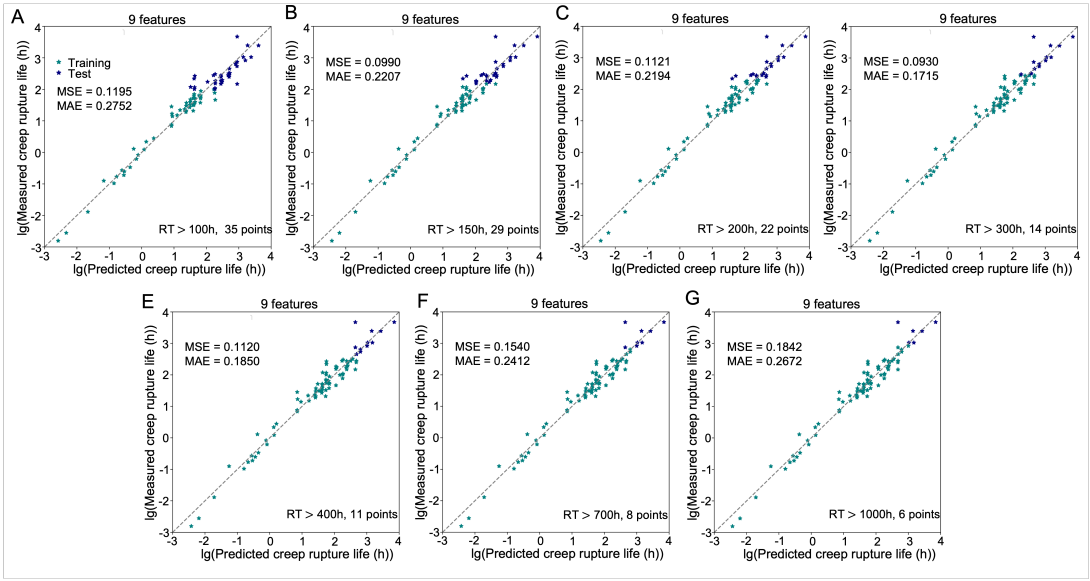

Figure 4. Extrapolation performance of the MLR models with nine features on the seven data divisions. (A) RT > 100 h; (B) RT > 150 h; (C) RT > 200 h; (D) RT > 300 h; (E) RT > 400 h; (F) RT > 700 h; and (G) RT > 1,000 h. MLR: Multiple linear regression; RT: creep rupture life.

intersection of the features from the seven data sets for further modeling. The intersection has nine features: solution_time, C, Ni, Nb+Ta, V, Fe, Sn, test_temperature, and test_stress. Using these nine features, we retrain the MLR models and examine their performance for the seven data sets, as shown in Figure 4. All the models still have superior performance in both training and testing data, confirming the robustness of the nine features for extrapolation.

The feature, solution_temperature, is removed due to the very small coefficient in all seven data divisions. In addition, it is noted that of the nine features, six are the contents of elements. To further simplify the MLR models, we transform the six elemental contents to a composition-based feature, the Molybdenum equivalent ($[Mo]_{eq}$), a well-known attribute used for the design of titanium alloys[45]. We reconstruct the MLR models using the three features: i.e., $[Mo]_{eq}$, test_temperature, and test_stress. Using the dataset with RT > 100 h as an example, the calculation of $[Mo]_{eq}$ and the learned formula are given by

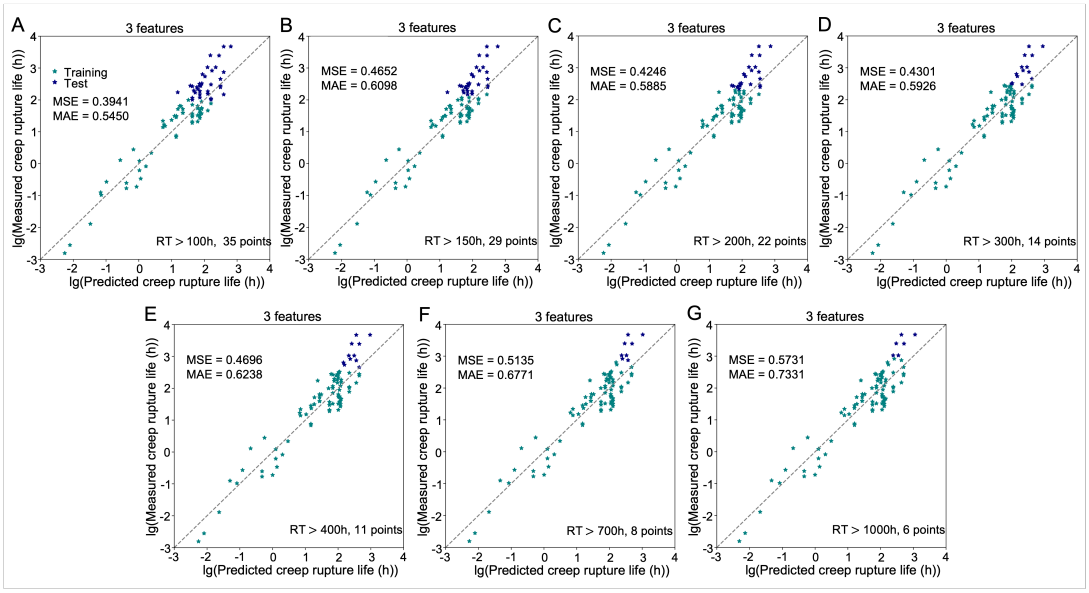

Figure 5. Extrapolation performance of the MLR models with three features on the seven data divisions. (A) RT > 100 h; (B) RT > 150 h; (C) RT > 200 h; (D) RT > 300 h; (E) RT > 400 h; (F) RT > 700 h; and (G) RT > 1,000 h. MLR: Multiple linear regression; RT: creep rupture life.

$$[Mo]_{eq} = 1.0\,Mo + 0.67\,V + 0.44\,W + 0.28\,Nb + 0.22\,Ta + 2.9\,Fe + 1.6\,Cr - 1.0\,Al \ (\text{mass\%}). \quad (6)$$

$$y = 5.952 - 4.519[Mo]_{eq} - 3.869 test\_temperature - 2.599 test\_stress. \quad (7)$$

Figure 5A-G shows the performance of the new MLR models. Compared to Figure 4, there is a slight degradation in model performance. This suggests that even with three features, we can obtain accurate formulae for extrapolated prediction of creep rupture life of high-temperature titanium alloys. To demonstrate the superiority of the MLR models, we also retrain the five black-box models for comparison, as shown in Figure 6. It is found that in all seven data division scenarios, MLR models always exhibit the lowest MSE and MAE metrics. An interesting observation is that the performance of MLR consistently outperforms CNN in Figure 6, whereas this is not the case in Figure 2. This can be attributed to the fact that the CNN model can generate information-rich features by the use of convolutional kernels on high-dimensional feature space; however, the only three retained features herein may not be adequate for training a robust CNN model.

3.3. Simple formulae for creep rupture life prediction

The MLR algorithm assumes a linear relationship between independent and dependent variables, and the resulting models (formulae) with three features demonstrate optimal performance in extrapolated predictions. However, there may exist nonlinearity in the high-temperature titanium alloy creep data, which deserves further exploration for improved formulae. The SISSO algorithm is employed to search for better formulae, which is realized by combining the three selected basic features with arithmetic operations. Such combinations may capture the possible nonlinear patterns behind the data and provide highly accurate formulae[46].

We apply SISSO to the seven datasets and identify the corresponding optimal 2D (two variables, x_1 and x_2) and 3D (three variables, x_1, x_2 and x_3) formulae for testing data, as listed in Table 1. The dimension can be further expanded for more accurate formulae, but we herein only consider the 2D and 3D ones that have relatively simple forms. It is seen that for different datasets, the 3D formulae do not necessarily outperform the 2D ones. The optimal formulae for each data set are highlighted in bold. All the formulae from SISSO have lower MSE and MAE than those from MLR models. The model improvement is particularly prominent for

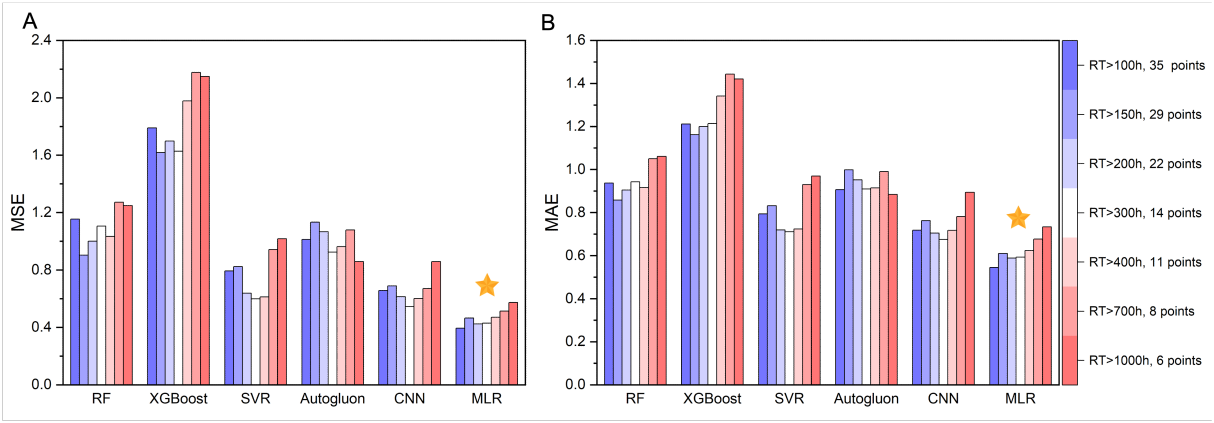

Figure 6. Comparison of model (based on three features) performances on different testing data sets. (A) MSE and (B) MAE. MSE: Mean squared error; MAE: mean absolute error.

Table 1. The 2D and 3D SISSO formulae under different data divisions, along with the metrics for these formulas compared to the MLR models (ts means test_stress and tt means test_temperature)

Dataset	a_0	a_1	x_1	a_2	x_2	a_3	x_3	MAE of SISSO	MSE of SISSO	MAE of MLR	MSE of MLR
RT100-Test	**6.7818**	**-4.1975**	$\boldsymbol{[Mo]_{eq}+ts}$	**-4.2051**	$\boldsymbol{tt}$			**0.3229**	**0.4950**	0.3941	0.5450
RT100-Test	5.3672	-4.6069	$[Mo]_{eq}$	-4.0322	$ts+tt$	0.8464	e^{ts}	0.3737	0.5232		
RT150-Test	**6.4416**	**-4.0672**	$\boldsymbol{[Mo]_{eq}+ts}$	**-3.8309**	$\boldsymbol{tt}$			**0.3920**	**0.5616**	0.4652	0.6098
RT150-Test	6.2814	-4.5942	$[Mo]_{eq}$	-3.8294	$ts+tt$	1.4103	ts^3	0.4260	0.5772		
RT200-Test	6.5681	-4.1523	$[Mo]_{eq}+ts$	-3.8479	tt			0.3233	0.5138	0.4246	0.5885
RT200-Test	**6.8009**	**-4.74158**	$\boldsymbol{[Mo]_{eq}+ts}$	**-4.0244**	$\boldsymbol{tt}$	**2.1151**	$\boldsymbol{ts^3}$	**0.3162**	**0.5055**		
RT300-Test	6.6401	-4.2067	$[Mo]_{eq}+ts$	-3.8421	tt			0.3062	0.5010	0.4301	0.5926
RT300-Test	**6.8709**	**-4.8060**	$\boldsymbol{[Mo]_{eq}+ts}$	**-4.0096**	$\boldsymbol{tt}$	**2.1381**	$\boldsymbol{ts^3}$	**0.3016**	**0.4854**		
RT400-Test	**6.7327**	**-4.2581**	$\boldsymbol{[Mo]_{eq}+ts}$	**-3.8982**	$\boldsymbol{tt}$			**0.2625**	**0.4584**	0.4696	0.6238
RT400-Test	6.9556	-4.8583	$[Mo]_{eq}+ts$	-4.0598	tt	2.1574	ts^3	0.3162	0.4042		
RT700-Test	**6.7670**	**-4.2891**	$\boldsymbol{[Mo]_{eq}+ts}$	**-3.9028**	$\boldsymbol{tt}$			**0.2919**	**0.4946**	0.5135	0.6771
RT700-Test	6.9949	-4.8912	$[Mo]_{eq}+ts$	-4.0664	tt	2.1492	ts^3	0.3401	0.4608		
RT1000-Test	6.8457	-4.3289	$[Mo]_{eq}+ts$	-3.9695	tt			0.2948	0.5130	0.5731	0.7331
RT1000-Test	**7.1073**	**-4.9436**	$\boldsymbol{[Mo]_{eq}+ts}$	**-4.1695**	$\boldsymbol{tt}$	**2.1454**	$\boldsymbol{ts^3}$	**0.2934**	**0.4529**		

The bolds mean the optimal formula for each dataset. RT100-Test indicates the testing data with RT > 100 h, similar to the others. More details of the formulae can be found from Methods. SISSO: Sure independence screening and sparsifying operator; MLR: multiple linear regression; MAE: mean absolute error; MSE: mean squared error; RT: creep rupture life.

the data set with RT > 400 h (RT400-Test), where the MSE and MAE are reduced by approximately 44% and 27%, respectively.

Note that although nonlinear arithmetic operations are involved in generating new features, the optimal 2D formulae we obtain contain only addition and the 3D formulae include only addition and exponentiation. Moreover, for all the seven datasets, the 2D formulae have the same x and the only differences lie in the coefficients. The three 3D formulae in bold have errors merely about 0.01 lower than those of the 2D formulae. To obtain a unified formula for all these seven datasets, we average the coefficients of the 2D formulae for the seven datasets and the corresponding formula is as below

$$y = 6.6824 - 4.2143([Mo]_{eq} + test\_stress) - 3.9275(test\_temperature) \quad (8)$$

We examine the efficacy of the above formula on the seven datasets, and the model performance is compared to optimal 2D and 3D formulae (bolds in Table 1) and the MLR models [Figure 7]. Figure 7 shows that the unified formula performs similarly to those from SISSO and better than those from MLR. However, it should

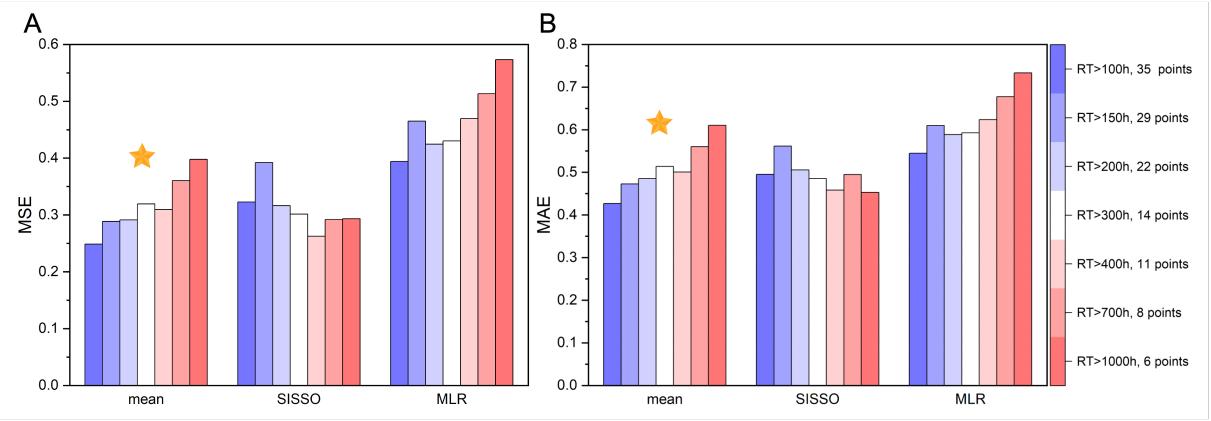

Figure 7. Comparing the SISSO and MLR-based formulae to the "mean" formula (based on three features) on different testing datasets. (A) MSE and (B) MAE. SISSO: Sure independence screening and sparsifying operator; MLR: multiple linear regression; MSE: mean squared error; MAE: mean absolute error.

be pointed out that the formulae from SISSO and MLR change with different training and testing data. By contrast, the final formula in Equation (8) has a fixed form and can be preferred by the materials community.

Traditionally, the TTP extrapolation methods have been used for predicting the long-term creep rupture life by fitting the measured short-term rupture life. These methods usually only consider the test_stress and test_temperature as inputs; thus, they are limited to a small subset of alloys where adequate experimental data are available. Here, in addition to test conditions, the learned formula also involves the composition-based $[Mo]_{eq}$ that often indicates the phase transition and stability of titanium alloys. As a result, it allows us to apply the unified formula to titanium alloys of various chemistries. Additionally, the learned formula considering $[Mo]_{eq}$ can be combined with optimization algorithms to not only further facilitate the design of new alloys with improved creep properties[47], but also aid in the clarification of the deformation mechanisms. It is intriguing to see that the learned simple formula outperforms the five black-box surrogate models, including the advanced automated ML and convolutional neural networks. The reason may lie in the linear-like trend between test conditions and creep rupture life for a given alloy[16,48], as generally the black-box algorithms are more flexible and often provide more accurate prediction models. For different data, various algorithms should be tried and then the proper one can be selected. That is, there is no universal algorithm for all kinds of data. Previous studies have also shown a similar phenomenon that the linear models perform better than black box models in extrapolation tasks[49,50].

4. CONCLUSIONS

In summary, we build a variety of ML models including both black-box and white-box ones, and compare their performance in predicting the long-term creep rupture life by learning from the short-term creep rupture life data of high-temperature titanium alloys. It is found that the MLR performs much better than the other five typical black-box surrogate models, even the advanced convolutional neural networks and automated ML. Feature selection by Lasso helps to further simplify the MLR-based model, but meanwhile the accuracy degenerates. This then motivates us to use symbolic regression to establish more accurate formulae with the selected three features, the Molybdenum equivalent, the test stress and test temperature. Finally, a quite simple but unified formula is obtained for accurate creep rupture life prediction of high-temperature titanium alloys.

DECLARATIONS

Authors' contributions

Made substantial contributions to conception and design of the study and performed data analysis and interpretation: Wang P, Zhao S, Zhou C, Yuan R

Performed data acquisition and provided administrative, technical, and material support: Fan J, Tang B, Li J, Yuan R

Availability of data and materials

The data and codes are uploaded to the author's github repository: https://github.com/nwpuai4msegroup/creep-rupture-life-prediction.

Financial support and sponsorship

This work was financially supported by the National Key Research and Development Program of China (2021YFB3702604).

Conflicts of interest

All authors declared that there are no conflicts of interest.

Ethical approval and consent to participate

Not applicable.

Consent for publication

Not applicable.

REFERENCES

1. Zhang Z, Fan J, Tang B, et al. Microstructural evolution and FCC twinning behavior during hot deformation of high temperature titanium alloy Ti65. *J Mater Sci Technol* 2020;49:56–69. DOI
2. Liu H, Wang H, Ren L, Qiu D, Yang K. Antibacterial copper-bearing titanium alloy prepared by laser powder bed fusion for superior mechanical performance. *J Mater Sci Technol* 2023;132:100–9. DOI
3. Gao P, Fu M, Zhan M, Lei Z, Li Y. Deformation behavior and microstructure evolution of titanium alloys with lamellar microstructure in hot working process: a review. *J Mater Sci Technol* 2020;39:56–73. DOI
4. Boyer RR. An overview on the use of titanium in the aerospace industry. *Mat Sci Eng A* 1996;213:103–14. DOI
5. Wu X, Makineni SK, Liebscher CH, et al. Unveiling the Re effect in Ni-based single crystal superalloys. *Nat Commun* 2020;11:389. DOI
6. Cui C, Hu BM, Zhao L, Liu S. Titanium alloy production technology, market prospects and industry development. *Mater Design* 2011;32:1684–91. DOI
7. Sattar M, Othman AR, Kamaruddin S, Akhtar M, Khan R. Limitations on the computational analysis of creep failure models: a review. *Eng Fail Anal* 2022;134:105968. DOI
8. Jelwan J, Chowdhury M, Pearce G. Design for creep: a critical examination of some methods. *Eng Fail Anal* 2013;27:350–72. DOI
9. Barboza MJR, Neto CM, Silva CRM. Creep mechanisms and physical modeling for Ti–6Al–4V. *Mat Sci Eng A* 2004;369:201–9. DOI
10. Bolton J. The potential for major extrapolation of creep rupture and creep strain data. *Mate High Temp* 2014;31:109–20. DOI
11. Bolton J. Reliable analysis and extrapolation of creep rupture data. *Int J Pres Ves Pip* 2017;157:1–19. DOI
12. MacLachlan DW, Knowles DM. Modelling and prediction of the stress rupture behaviour of single crystal superalloys. *Mat Sci Eng A* 2001;302:275–85. DOI
13. Prasad SC, Rajagopal KR, Rao IJ. A continuum model for the anisotropic creep of single crystal nickel-based superalloys. *Acta Mater* 2006;54:1487–500. DOI
14. Oruganti R, Karadge M, Swaminathan S. Damage mechanics-based creep model for 9–10% Cr ferritic steels. *Acta Mater* 2011;59:2145–55. DOI
15. Zhang K, Tan JP, Sun W, Nikbin K, Tu ST. Determination of multiaxial stress rupture criteria for creeping materials: a critical analysis of different approaches. *J Mater Sci Technol* 2023;137:14–25. DOI
16. Larson FR, Miller J. A time-temperature relationship for rupture and creep stresses. *Trans ASME* 1952;74:765–71. DOI
17. Dyson BF. Microstructure based creep constitutive model for precipitation strengthened alloys: theory and application. *Mater Sci Technol* 2009;25:213–20. DOI

18. Zhou H, Li J, Liu J, et al. Significant reduction in creep life of P91 steam pipe elbow caused by an aberrant microstructure after short-term service. *Sci Rep* 2024;14:5216. DOI
19. Dang YY, Zhao XB, Yuan Y, et al. Predicting long-term creep-rupture property of Inconel 740 and 740H. *Mater High Temp* 2016;33:1–5. DOI
20. Kim WG, Yin SN, Lee GG, Kim YW, Kim SJ. Creep oxidation behaviour and creep strength prediction for Alloy 617. *Int J Press Ves Pip* 2010;87:289–95. DOI
21. Vladimirov IN, Reese S, Eggeler G. Constitutive modelling of the anisotropic creep behaviour of nickel-base single crystal superalloys. *Int J Mech Sci* 2009;51:305–13. DOI
22. Hart GLW, Mueller T, Toher C, Curtarolo S. Machine learning for alloys. *Nat Rev Mater* 2021;6:730–55. DOI
23. Shin D, Yamamoto Y, Brady MP, Lee S, Haynes JA. Modern data analytics approach to predict creep of high-temperature alloys. *Acta Mater* 2019;168:321–30. DOI
24. Zhou CL, Yuan RH, Liao WJ, et al. Creep rupture life predictions for Ni-based single crystal superalloys with automated machine learning. *Rare Met* 2024;43:2884-90. DOI
25. Mamun O, Wenzlick M, Sathanur A, Hawk J, Devanathan R. Machine learning augmented predictive and generative model for rupture life in ferritic and austenitic steels. *Npj Mat Degrad* 2021;5:20. DOI
26. Chen C, Wang Q, Dong C, Zhang Y, Dong H. Composition rules of Ni-base single crystal superalloys and its influence on creep properties via a cluster formula approach. *Sci Rep* 2020;10:21621. DOI
27. Ramprasad R, Batra R, Pilania G, Mannodi-Kanakkithodi A, Kim C. Machine learning in materials informatics: recent applications and prospects. *npj Comput Mater* 2017;3:54. DOI
28. Butler KT, Davies DW, Cartwright H, Isayev O, Walsh A. Machine learning for molecular and materials science. *Nature* 2018;559:547–55. DOI
29. Biswas S, Fernandez Castellanos D, Zaiser M. Prediction of creep failure time using machine learning. *Sci Rep* 2020;10:16910. DOI
30. Venkatesh V, Rack HJ. A neural network approach to elevated temperature creep–fatigue life prediction. *Int J Fatigue* 1999;21:225–34. DOI
31. Liu Y, Wu J, Wang Z, et al. Predicting creep rupture life of Ni-based single crystal superalloys using divide-and-conquer approach based machine learning. *Acta Mater* 2020;195:454–67. DOI
32. Zhou C, Yuan R, Su B, et al. Creep rupture life prediction of high-temperature titanium alloy using cross-material transfer learning. *J Mater Sci Technol* 2024;178:39–47. DOI
33. Ouyang R, Curtarolo S, Ahmetcik E, Scheffler M, Ghiringhelli LM. SISSO: a compressed-sensing method for identifying the best low-dimensional descriptor in an immensity of offered candidates. *Phys Rev Mater* 2018;2:083802. DOI
34. Evans RW, Hull RJ, Wilshire B. The effects of alpha-case formation on the creep fracture properties of the high-temperature titanium alloy IMI834. *J Mater Proc Technol* 1996;56:492–501. DOI
35. Zheng Z, Xiao S, Wang X, et al. High temperature creep behavior of an as-cast near-α Ti–6Al–4Sn–4Zr-0.8 Mo–1Nb–1W-0.25 Si alloy. *Mat Sci Eng A* 2021;803:140487. DOI
36. Mishra H, Ghosal P, Nandy TK, Sagar PK. Influence of Fe and Ni on creep of near α-Ti alloy IMI834. *Mat Sci Eng A* 2005;399:222–31. DOI
37. Zheng Z, Kong F, Chen Y, Wang X. Effect of nano-Y_2O_3 addition on the creep behavior of an as-cast near-α titanium alloy. *Mater Charact* 2021;178:111249. DOI
38. Li W, Chen Z, Liu J, Wang Q, Sui G. Effect of texture on anisotropy at 600 °C in a near-α titanium alloy Ti60 plate. *Mat Sci Eng A* 2017;688:322–9. DOI
39. Briguente LANS, Couto AA, Guimarães NM, Reis DAP, de Moura Neto C, Barboza MJR. Determination of creep parameters of Ti-6Al-4V with bimodal and equiaxed microstructure. In: Defect Diffus Forum. 2012;326-8:520–4. DOI
40. Singh G, Satyanarayana DVV, Pederson R, Datta R, Ramamurty U. Enhancement in creep resistance of Ti–6Al–4V alloy due to boron addition. *Mat Sci Eng A* 2014;597:194–203. DOI
41. Oliveira VMCA, Vazquez AM, Aguiar C, Robin A, Barboza MJR. Nitride coatings improve Ti-6Al-4V alloy behavior in creep tests. *Mat Sci Eng A* 2016;670:357–68. DOI
42. Zhang Z, Fan J, Li R, et al. Orientation dependent behavior of tensile-creep deformation of hot rolled Ti65 titanium alloy sheet. *J Mater Sci Technol* 2021;75:265–75. DOI
43. Omprakash CM, Satyanarayana DVV, Kumar V. Effect of primary α content on creep and creep crack growth behaviour of near α-Ti alloy. *Mater Sci Technol* 2011;27:1427–32. DOI
44. Erickson N, Mueller J, Shirkov A, et al. AutoGluon-tabular: robust and accurate automl for structured data. arXiv. [Preprint.] Mar 13, 2020 [accessed 2024 Nov 15]. Available from: https://doi.org/10.48550/arXiv.2003.06505.
45. Weiss I, Semiatin SL. Thermomechanical processing of beta titanium alloys - an overview. *Mat Sci Eng A* 1998;243:46–65. DOI
46. Makke N, Chawla S. Interpretable scientific discovery with symbolic regression: a review. *Artif Intell Rev* 2024;57:2. DOI
47. Yang F, Li Z, Wang Q, et al. Cluster-formula-embedded machine learning for design of multicomponent β-Ti alloys with low Young's modulus. *npj Comput Mater* 2020;6:101. DOI
48. Monkman FC. An empirical relationship between rupture life and minimum creep rate in creep-rupture tests. 1956. pp. 593–620. Available from: https://api.semanticscholar.org/CorpusID:222409633. [Last accessed on 15 Nov 2024]
49. McCartney M, Haeringer M, Polifke W. Comparison of machine learning algorithms in the interpolation and extrapolation of flame describing functions. *J Eng Gas Turbines Power* 2020;142:061009. DOI

50. Muckley ES, Saal JE, Meredig B, Roper CS, Martin JH. Interpretable models for extrapolation in scientific machine learning. *Digit Discov* 2023;2:1425–35. DOI